CONVERGENCE ASSESSMENT IN EULERIAN FLUIDIZED BED SIMULATION

Luciano Bernardes Diettrich, luciano.diettrich@gmail.com
Horácio Antonio Vielmo
Department of Mechanical Engineering – Federal University of Rio Grande do Sul

Abstract. *The formulation of the fluidized bed models and its flow characteristics make the answers strongly dependent of the discretization parameters and sensitive to the uncertainty sources. The study of different errors sources to the results is done, to individualize probable causes of the non-asymptotic, non-monotonic or oscillating results with the discretization variation. The case is a bi-dimensional two-phase transient flow, with an Eulerian model. The simulations were verified; the error band was calculated with the GCI. It has seen that the grid convergence curve is not monotonic. In the bed surface (between the solid material and the region with only gas) and inside the bubbles there is a high volume fraction gradient, which generates a numerical oscillation. The generated perturbation in the answer is carried forward through the time steps and it generates oscillations in the velocities and different variations in the volume fraction. A polynomial regression is suggested, which is a more flexible tool than the Richardson Extrapolation to the answers with errors. The value of R^2 is a good indicative of the answer errors, being a useful parameter to evaluate 3 or more grids. The GCI and the R^2 vary along the time.*

Keywords: *Fluidization, Fluidized bed, GCI, Richardson Extrapolation, numerical error, transient CFD*

1. INTRODUCTION

Some mathematical models were created with the specific purpose of representing the physical behavior of the dynamics of fluidized bed. These models have been validated for some years; however there are still gaps in its study.

The rapid development of computers has made possible more complex models of fluid dynamics, while access to these computational tools has been easier, for these reasons assessment techniques to the uncertainty in results, becoming more important. Despite its formulation sensitive to errors, the current scientific publications dealing with models for fluidized beds does not take into account the discretization parameters through a detailed study. Without these detailed studies, is created confusion between the correct numerical solution of the problem and what would be a wrong solution to this, under inaccurate conditions.

This work studies the convergence, with the change in grid size on models for numerical simulation of fluidized beds. The Grid Convergence Index (GCI) is used to estimate the range of results errors and some parameters of polynomial regression to assess the numerical results obtained at different times. The assessment of the sources of errors on the response of the problem is held in order to identify probable reasons for results non-asymptotic, not monotonous or oscillating with discretization refinement.

2. NUMERIC SIMULATION MODELS

The simulations were carried out with the commercial code Fluent 6.3, using only the existing formulation in it. It's a transient, biphasic and bi-dimensional flow; following an Eulerian model.

2.1. Governing Equations

The equations of mass conservation and momentum for Eulerian model of two species appear below.

Conservation of mass:

Gas phase:

$$\frac{\partial(\varepsilon_f \rho_f)}{\partial t} + \nabla \cdot (\varepsilon_f \rho_f \overline{u}) = 0 \tag{2.1}$$

Solid phase:

$$\frac{\partial(\varepsilon_s \rho_s)}{\partial t} + \nabla \cdot (\varepsilon_s \rho_s \overline{v}) = 0 \tag{2.2}$$

Conservation of momentum

Gas phase:

$$\frac{\partial(\varepsilon_f \rho_f \overline{u})}{\partial t} + \nabla \cdot (\varepsilon_f \rho_f \overline{u}\overline{u}) = \varepsilon_f \nabla p - \beta(\overline{u} - \overline{v}) - (\nabla \cdot \varepsilon_f \tau_f) + \varepsilon_f \rho_f g \tag{2.3}$$

Solid phase:

$$\frac{\partial(\varepsilon_s \rho_s \overline{v})}{\partial t} + \nabla \cdot (\varepsilon_s \rho_s \overline{v}\overline{v}) = \varepsilon_s \nabla p + \beta(\overline{u} - \overline{v}) - (\nabla \cdot \varepsilon_s \tau_s) - \nabla p_s + \varepsilon_s \rho_s g \tag{2.4}$$

The inter-phase momentum transfer is an important term for modeling interaction gas-solid, because the fluidization is a result of the drag exercised by interstitial gas in solid phase. This drag is modeled through the semi-empirical, transfer inter-phase momentum coefficient β , which is modeled with the model from Gidaspow (1992).

$$\beta = 150 \frac{\varepsilon_s^2}{\varepsilon_f} \frac{\mu_f}{d_p^2} + 1{,}75 \varepsilon_s \frac{\rho_f}{d_p} \left| \bar{u} - \bar{v} \right| , \ \varepsilon_f \le 0{,}80 \qquad (2.5)$$

$$\beta = \frac{3}{4} C_d \varepsilon_s \frac{\rho_f}{d_p} \left| \bar{u} - \bar{v} \right| \varepsilon_s^{-1{,}65} , \qquad \varepsilon_f > 0{,}80 \qquad (2.6)$$

Where:

$$C_d = \frac{24}{\mathrm{Re}_p} \left(1 + 0{,}15 \left(\mathrm{Re}_p \right)^{0{,}687} \right) \qquad (2.7)$$

$$\mathrm{Re}_p = \frac{\rho_f \left| \bar{u} - \bar{v} \right| d_p}{\mu_f} \qquad (2.8)$$

The biphasic model presented needs constituent equations to describe the solid phase rheology. The viscosity of solid phase describes the internal transfer of momentum due to shear stress, and the pressure gradient resulting from normal stress interaction between the particles. The particles have a random movement, and the velocities fluctuation creates an effective pressure, with an effective viscosity (because of the resistance movement in the regions of shear between particles).

The rheological properties of solid phase are calculated based on the local concentration and fluctuation of the movement because of collisions between particles. Linked to movement of random particles, a pseudo-temperature Θ_s can be defined as $\frac{3}{2}\Theta_s = \frac{1}{2}\overline{C_s \cdot C_s}$, with C_s the randomly velocity fluctuating of the solid phase. An additional transport equation for the kinetic energy is used to describe the random distribution of granular temperature.

$$\frac{3}{2}\left\{ \frac{\partial}{\partial t}\left(\varepsilon_s \rho_s \Theta_s \right) + \nabla \cdot \left(\varepsilon_s \rho_s \Theta_s \bar{v} \right) \right\} = \underbrace{-\left(p_s \bar{\bar{I}} + \varepsilon_s \tau_s \right) : \nabla \cdot \bar{v}}_{\text{energy generation of solid phase stress tensor}} + \overbrace{\nabla \cdot \left(k_s \nabla \Theta_s \right)}^{\text{solid phase kinetic energy diffusion}} \underbrace{- \gamma}_{\text{collision energy dissipation}} \overbrace{- 3 \beta \Theta_s}^{\text{inter-phase energy transfer.}} \qquad (2.9)$$

The solver used is segregated, the conservation equations for each phase are resolved separately, the variable to be calculated in each cell uses known and unknown values of surrounding cells, the unknown values appear in the equations of different cells, while being resolved.

Two different advective-difusives interpolation functions are used: second order Upwind for the equations of momentum conservation and granular temperature and first order Upwind for volume fraction. The discretization time is made with a first order implicit model.

3. CHECKING THE SIMULATION

According to the AIAA (1998), verification is the process of determining that a model implementation accurately represents the developer's conceptual description of the model and the solution to the model. The study for verification can be carried out with different purposes: verification of the model, code verification or verification of a simulation. In this case are considered valid the results obtained in earlier works for the validation of models and the code, as in Patil et al (2005) and Boemer et al (1998). This work has been designed to verify the simulation and to calculate the uncertainty of the solution with error estimation tools as the GCI (Grid convergence index).

3.1. Sources of simulation errors

The numerical error of a variable of interest is the difference between its exact analytical solution and its numerical solution, according to Ferziger and Peric (1999). The exact analytical solution usually is unknown, but it will be equal to the numerical solution with zero error. The purpose of verification is to determine whether a mathematical model is being accurately resolved by a numerical method.

The numerical errors can be caused by different sources; in this work it is considered the next three errors:

a.) Discretization errors: are those errors that occur from the representation of the governing flow equations and other physical models as algebraic expressions in a discrete domain of space and time. This error reduces by reducing the characteristic size of the discretization (time step or element size).

b.) Iterative convergence error: is the difference between the value at some iteration and the exact value. This error tends to decrease by increasing the number of iterations, i.e. reducing the convergence criteria.

c.) Computer round-off errors: caused by the representation of floating point numbers on the computer and depend on the accuracy at which numbers are stored. This error increases with smaller elements, but usually is less significant.

An approximated theoretical curve of convergence is built, in Figure 3.1; this is a hypothetical convergence curve in terms of element characteristic size, with the shaded area representing the limit of error in the solution.

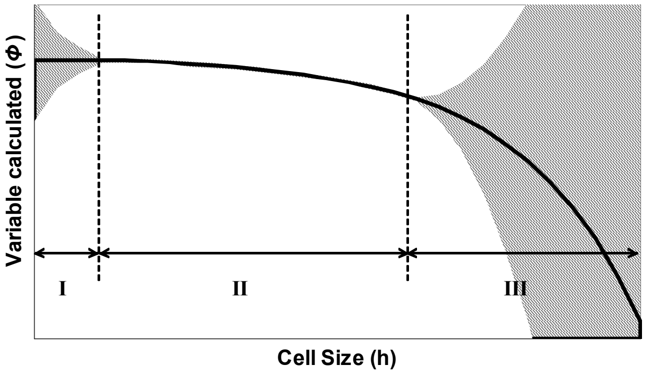

Figure 3.1: Convergence characteristic curve.

The region I is characterized by the error (c), related to computer round-off, increasing with smaller elements. The region II is the piece where only the error (a) is relevant, other errors are less important. In this excerpt the flow phenomena are already captured, but can still be poorly characterized, is the region where shall be made the convergence study by generalized Richardson extrapolation. The region III presents the errors (a) and (b) amplified by diffusion or numerical oscillation (more relevant in the case of highly convective flows), due to the largest element, the errors amplify, and some scales of the phenomena are not captured, making the answers untrustworthy.

3.2. Grid Convergence Index

The spatial verification of convergence is a way to determine the error due to finite domain discretization. Such verification is known as grid convergence study or grid refinement study. The methodology of analysis involves performing the simulation in two or more different meshes, successively more refined. With the grid refinement (reducing the geometric size of the cells and increasing the total cells number) or with time step decreases, the discretization errors asymptotically approaches zero.

Methods for evaluation time and space convergence were presented by different authors. According Roache (1993), there is inconsistency and confusion in some works that deal with the grid convergence. That is the motivation for the development of the grid convergence Index (GCI). The evaluation of the grid convergence allows determining a range of error for the studied variable and also to obtain an estimation of the exact solution value of the problem. The GCI of a particular variable under study is given by:

$$GCI = F_s \frac{|\varepsilon_h|}{r^{p_h} - 1} \tag{3.1}$$

With:

$$r = \left(\frac{N_1}{N_2}\right)^{1/D} = \frac{h_2}{h_1} \tag{3.2}$$

$$\varepsilon_h = \frac{\phi_2 - \phi_1}{\phi_1} \tag{3.3}$$

Where r is the effective grid refinement ratio, $\boldsymbol{N}$ is the total number of grid points used for the grid, $\boldsymbol{D}$ is the dimension of the flow domain, $\boldsymbol{p_h}$ is the order of convergence and ε_h represents the standard error between a generic calculated variable ϕ. The index 1 refers to the finer grid and the index 2 refers to the coarser grid. The security factor F_s will be 3 as recommended by Roache (1993), for all cases calculated in this work.

3.3. Richardson Extrapolation

Richardson extrapolation is a method for obtaining a higher-order estimate of the continuum value ϕ_{exact} (value at zero grid spacing) from a series of lower-order discrete values. A simulation with grid spacing h, will result in a value

ϕ of any variable. This variable can be expressed by the series expansion, with a constant K_i (independent of h) and the order of convergence $\boldsymbol{p_h}$:

$$\phi_{exact} = \phi(h) + K_0 h^{p_h} + K_1 h^{p_h+1} + K_2 h^{p_h+2} + \ldots \tag{3.4}$$

The term of lower order ($\boldsymbol{p_h}$) is more relevant, the other terms are included in HOT, or high order terms, and it is considered $K_0 = K$. So the equation 3.4 can be presented as the equation 3.5. Using up solutions of consecutive meshes ϕ_1 and ϕ_2, considering the refinement ratio r, and neglecting the HOT, the equation 3.5 results the equation 3.6, which relates to the exact solution: two consecutive solutions, refinement ratio and order of convergence, this equation is called for Roache (1993) the Generalized Richardson Extrapolation.

$$\phi_{exact} = \phi(h) + K h^{p_h} + H.O.T \tag{3.5}$$

$$\phi_{exact} = \phi_1 + \frac{\phi_1 - \phi_2}{r^{p_h} - 1} \tag{3.6}$$

3.4. Polynomial Regression

The Richardson Extrapolation takes into account that both consecutive solutions do not present any error than the discretization error (considers the grid convergence perfectly monotonous). One can, however, face different kinds of errors, such as numerical errors or incomplete convergence, which generate, even if in smaller-scale, disturbance of the convergence, making the values calculated for GCI inconsistent.

To take into account the possibility of errors from different sources, it was decided to approximate a curve through polynomial regression. The curve to be interpolated should follow the equation 3.5 with the HOT very small, which is monotonous and dependent only on h. For the numerical scheme used (Upwind of the second-order), it is known that the order of convergence p_h will be equal to 2, according to Marchi and Hobmeir (2007) and Demuren and Wilson (1993). Considering an estimated variable given for the fitted curve $\phi_{est}(h)$ placing the calculated variable $\phi(h)$, the equation 3.5 is reduced to equation 3.7

$$\phi_{est}(h) = \phi_{exact} + K h^2 \tag{3.7}$$

According to Rosseto (2006), the polynomial regression finds the curve that represents the given points with the lower total error possible. It is calculated the constants values for which the derivative of the sum of the square errors is zero.

$$\frac{\partial \sum_1^n (\phi_{est}(h_i) - \phi_i)^2}{\partial \phi_{exact}} = 0 \tag{3.8}$$

$$\frac{\partial \sum_1^n (\phi_{est}(h_i) - \phi_i)^2}{\partial K} = 0 \tag{3.9}$$

The value ϕ_i is the result of the simulation to the mesh i, with a respective h_i. The value of i is an integer number representing the level of mesh, from 1 for the finer grid, to n for the coarser grid. As seen in section 3.1, the errors not exclusively related to discretization increase with larger elements, i.e. more refined meshes have minor disruptions due to numerical sources and phenomena not captured, so it was decided to develop a weighted polynomial regression. Each point from the simulation will be linked to a weight value, which corresponds to the number of times that the point will be considered in the calculation of regression, for example, for a given mesh it was decided to assign a value of weight $\alpha_i = 6$, which means that the point on that mesh is 6 times in this polynomial regression, or as if there were 6 points equal to the this point. With this consideration, and with some mathematical operation with the equations 3.8 and 3.9, the relations 3.10 and 3.11 are reached, for ϕ_{exact} and K with the lowest total error.

$$\phi_{exact} = \left(\sum_1^n \alpha_i \phi_i \sum_1^n \alpha_i h_i^4 - \sum_1^n \alpha_i h_i^2 \sum_1^n \alpha_i h_i^2 \phi_i \right) \left(\sum_1^n \alpha_i \sum_1^n \alpha_i h_i^4 - \left(\sum_1^n \alpha_i h_i^2 \right)^2 \right)^{-1} \tag{3.10}$$

$$K = \left(\sum_1^n \alpha_i \sum_1^n \alpha_i h_i^2 \phi_i - \sum_1^n \alpha_i h_i^2 \sum_1^n \alpha_i \phi_i \right) \left(\sum_1^n \alpha_i \sum_1^n \alpha_i h_i^4 - \left(\sum_1^n \alpha_i h_i^2 \right)^2 \right)^{-1} \tag{3.11}$$

To evaluate the function of interpolation to the dispersion of data, it is used the correlation coefficient R^2, which varies from 0 to 1, whereas the closer to 1 is the R^2 lower is the error, i.e. the difference between the estimated value by the function and value obtained in the simulation. Based on the equation of the correlation coefficient presented in Rosseto (2006), it comes to the following equation, where $\overline{\phi}$ is the weighted average by α_i of the variable of study, and ϕ_{est} the estimated variable value.

$$R^2 = \left(\sum_1^n \alpha_i \left(\phi_{est}(h_i) - \phi_i \right)^2 \right) \left(\sum_1^n \alpha_i \left(\phi_i - \overline{\phi} \right) \right)^{-1} \tag{3.12}$$

If we consider a case with only two results ϕ_1 e ϕ_2, of two grids, and the refinement ratio $r = {}^{h_2}\!/_{h_1}$, the equation 3.10 is reduced to the Generalized Richardson Extrapolation (equation 3.6), becoming independent of the weight constants. In this case the correlation coefficient R^2 will be equal to 1, which shows that the Generalized Richardson Extrapolation will be a particular case with only two points for the polynomial regression. In the case where the answer is perfectly monotonous and the results in all meshes perfectly fit the curve of convergence, the result using the extrapolation of Richardson or polynomial regression will be identical and independent of weight constants, but if any of the results in a study suffer any disruption due to errors not related exclusively to discretization, the result of Richardson Extrapolation will not be accurate and may understate the error.

Using this model, the GCI will be given to the estimated value by the polynomial regression function (GCI_{est}), added to the relative error between estimated value ϕ_{st} and actual value ϕ.

$$GCI = GCI_{est} + \left| \frac{\phi - \phi_{est}}{\phi} \right| \tag{3.13}$$

4. SIMULATION PARAMETERS

The geometry studied was chosen because of various work already carried out with the same domain as in Boemer et al (1998), Patil (2005a) and Patil (2005b), and allows comparison with others CFD results or experimental results.

The studied case is a bi-dimension domain, basically a rectangle of 0.57m width and height of 1m, with the inlet at the bottom, outlet at the top and the sides are walls.

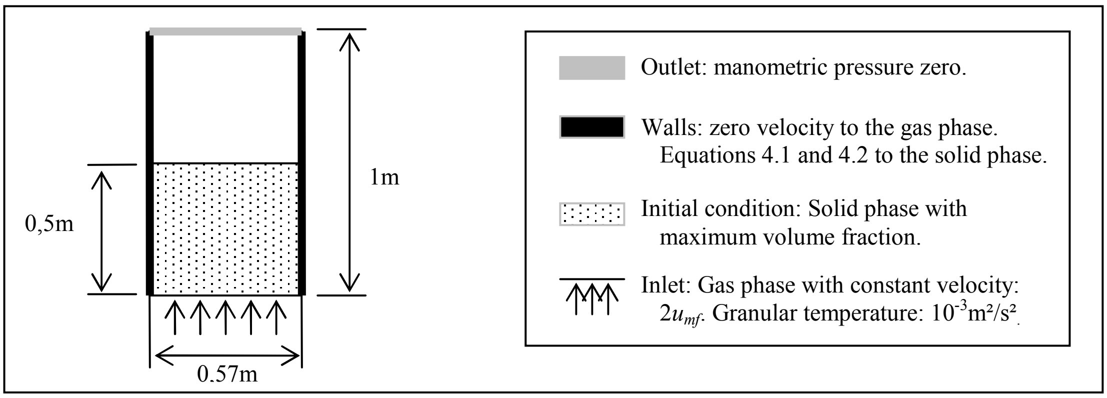

Figure 4.1: Geometry and boundary and initial conditions.

Table 4.1: Materials properties.

Particle diameter (d_p)	500 μ m	Restitution coefficient of walls (e_w)	0,2
Solid particle density (ρ_s)	2660 kg/m^3	Gas density (ρ_g)	1,2 kg/m³
Maximum volume fraction ($\varepsilon_s^{\max}$)	0,643569	Gas viscosity (μ_g)	1,85x10^{-5}kg/ms
Restitution coefficient (e)	0,9	Minimum fluidization velocity (u_{mf})	0,222 m/s

The boundary condition to the solid phase at the walls, is calculated from a microscopic model for collisions between particles and wall, according Sinclar and Jackson (1989).

In the meshes of this work were used quadrilateral elements, parallel to the geometry of the domain and identical elements in all domain, and keep up the aspect ratio (height / width) of the elements in all meshes. According to Demuren and Wilson (1993), the aspect ratio of the element may have strong influence on the response.

The sequence of grids follows a refinement ratio $r = 1.5$, and starts with a coarser grid with 32x64 cells, resulting in a series of 6 meshes with 2048, 4608, 10368, 23328, 52488 and 118098 elements.

5. RESULTS AND DISCUSSION

Various simulations were conducted to analyze the grid convergence. It was used a convergence criteria of 10^{-5}, due to the reduction of error. The simulations convergence curve is not monotonous for the grid refinement, the curve has a random oscillation.

Since this is a transient event, there is the possibility of an error due to discretization time, however, according to Roache (1993), time convergence and grid convergence are independent. It was used, in all cases, the same time step, and the answer may not suffer any disruptions due to the temporal convergence.

There is also the possibility of error propagation due to incomplete convergence, because the convergence criteria too high. But for that case it was used convergence criteria of 10^{-5}, which guarantees very low order of errors.

Another possibility is that error be related to numerical oscillations. As presented in Maliska (1995), numerical oscillations appear in cases with high gradients. It is known that in supersonic flows with the presence of shocks, are characterized strong gradients of pressure and in flows with not pre-mixed combustion there are large concentration gradients. Both flows have numerical fluctuations due to high gradients, and these kinds of flows suffer numerical oscillations.

From the analysis of the results, it was noted that in fluidized beds flow a region with a high gradient of volume fraction appears, this region is located in the interface between the bed of solid material and the region with just the gas phase. This abrupt change creates a strong numerical oscillation in the velocities.

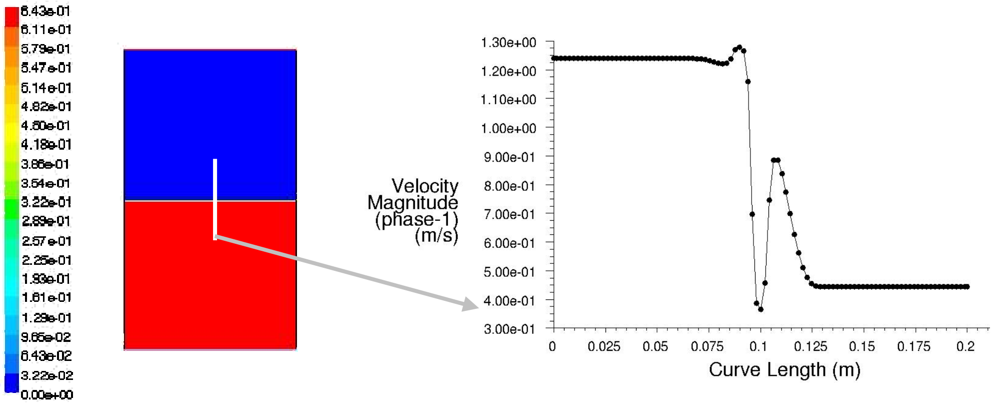

Figure 5.1: Position of the examined line in the domain with volume fraction of solid plotted (left) and the vertical velocity of the gas depending on the length of the examined line (right). 243x486 elements mesh in time 1×10^{-4}s.

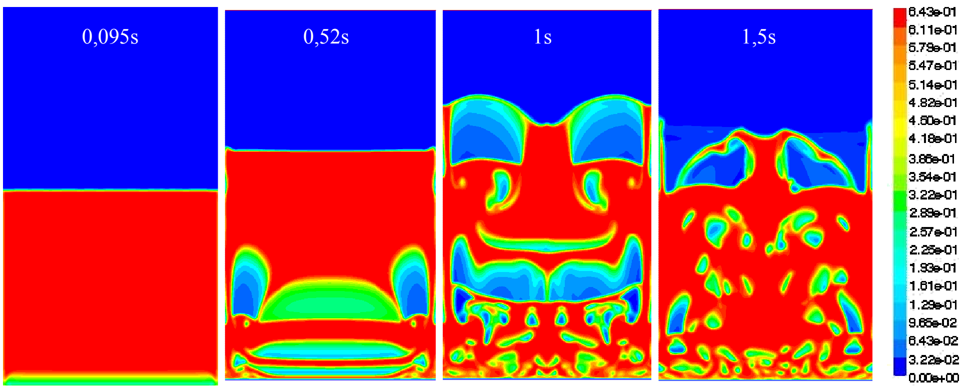

Figure 5.2: Distribution of volume fraction of solid for 162x324 elements mesh in time: 0,095s; 0,52s; 1s and 1,5 s.

In Figure 5.2 see that there is an expansion of bed in time and there is a distribution of volume fractions less abrupt in the interface region (because of the velocity fluctuations and because of the bubbles reach the surface). The process of bubbles formation is already started from about 0,3s; these bubbles have internal high gradients of volume fraction, which also generates dispersion of results of speed. The solution is apparently symmetrical, however, note that the result symmetries decreases along the time.

There are recent works that show the same effect on other types of flows, even for Upwind schemes and for high order schemes, as in Sjögreen (2003), where the author suggests a code filter, capable of capturing and reduce numeric fluctuations, enabling a study of convergence of mesh.

The characterization of numerical oscillations is very difficult, because it presents a random for different meshes and different times, and appears in different regions after the start of the formation of bubbles. So it was decided to use the correlation coefficient R^2 to assess the effect of fluctuations on the results, and the approximation 3.13 for the GCI. The progress of R^2 and the GCI for different meshes over time were studied. For the polynomial regression calculations it was used the weight constants $\alpha_1 = 6$, $\alpha_2 = 5$, $\alpha_3 = 4$ ... $\alpha_6 = 1$ respectivily to the six meshes, given the greater weight to the finest mesh.

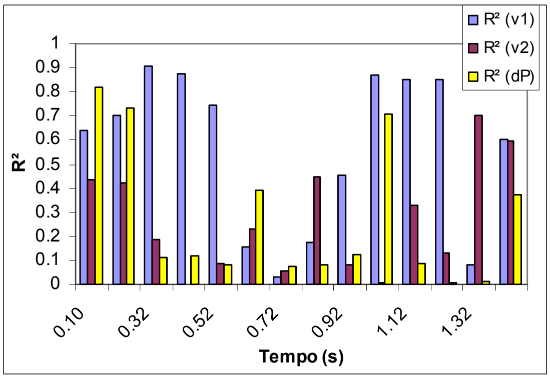

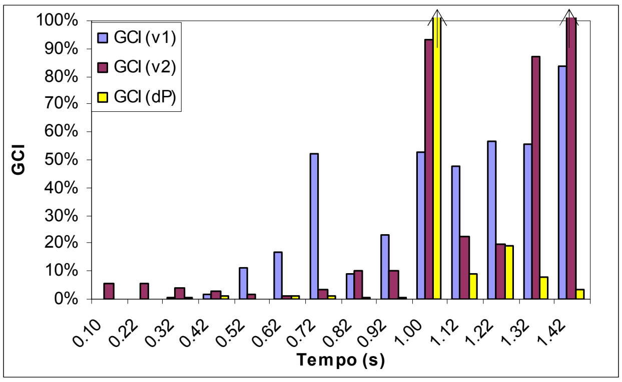

Figure 5.3: Progress of R^2 and the GCI over time to the mesh 243x486, both for the vertical velocity (v) of the gas in points 1 and 2 and the pressure drop of the system (dP).

Two points were studied, the point 1 is positioned at the ¼ of the geometry height and point 2 at ¾ of the geometry height, both positioned in vertical midline of the domain In Figure 5.3, the correlation coefficient R^2 to the point 1, decreases from 0,32s and presents a significant decrease after 0,52s (indicating greater dispersion of results) . About 0.32s the formation of bubbles begins, while around 0,52s the first bubble reaches the point 1. From 0,82s the bubbles just below the point 1 tends to decrease, decreasing the oscillation of velocity at this point.

The R^2 of the velocity at point 2 is initially low and decreases until 0,42s, which occurs because this point is more affected by the initial numerical oscillation, due the downstream position related to the interface, because the initial oscillation is generated to the interface gradient and gets less abrupt with the bed expansion. However, around 0,3s begins the formation of bubbles, and the velocity oscillations in the middle line (upstream the point 2) start to increase (decreasing R^2) from 0.62 s, making the response unstable.

The pressure drop of the system is the result of viscous friction, depending directly of the velocity distributions, leading to pressure to be a dependent variable of all velocity oscillations in the system, with a value of R^2 lower after the bubble formation, indicating a greater disruption in the velocity distribution.

Even in Figure 5.3 note that the GCI varies greatly over time, apparently growing. As a result for a specific mesh (162x324) and being a value of error range that takes into account the result distance from the exact value, in addition to the dispersion error, it is not clear direct effects of fluctuations on GCI values. However note that the GCI varies over time, which make impossible an analysis of grid convergence in time shorter than the total time of simulation, with the objective of make faster analysis to pre-select the necessary mesh. The GCI estimated for the pressure drop of the system is lower, indicating a minor grid dependence of this parameter.

6. CONCLUSIONS

In the fluidized bed flow there is a region with a high gradient of volume fraction located, initially, at the interface between the bed of solid material and the region with just the gas phase. This gradient creates a strong numerical oscillation in the gas phase velocities, as shown in Figure 5.1. The gas passes through the region with the highest volume fraction (solid bed) and goes to the region with zero volume fraction, which is equivalent to a duct abrupt expansion of almost twice of section. However, the cross section of the geometry is constant and there are not regions to form vortex. In the real flow or in a simulation that take into account the geometry of the particles, arise the effect of vortex formation just above the solid particles, similar to an outlet on spheres.

At the beginning of the process have only a bed expansion, and during this stage the gradient of volume fraction remains very high (on the surface of the bed), resulting in an abrupt change in the area equivalent of gas passage. This abrupt change decreases with the expansion of bed and with the explosion of the first bubbles on the surface. However, when starting the process of formation of bubbles, other high gradients are formed internally to bubbles, generating more errors.

The disturbance generated in results is carried forward through the time steps. Over time, after the bubbles start to reach the surface, it tends to reduce fluctuations, because the gradients of volume fraction internally to bubbles are smaller and tend to remain after the bubble explosion in the surface. However, the total area of regions with numerical oscillations changes due to the bubble formation, varying the numerical error in the solution, along the time.

The complex mathematical models formulation used tend to spread the error and may amplify them for some variables. The model of Gidaspow, used to model the interface transfer of momentum, has different formulations for different volume fractions, which leads to the answer differs from the convergence curve, for distributions of volume fraction not well-developed.

The use of polynomial regression has proven useful in this case as it presents a more flexible response to the analysis of errors, unlike the formulation of Richardson. The value of R^2 was a good indication of the influence of errors on the answer, and a very helpful parameter to assess a series with 3 or more grids.

4. REFERENCE

American Institute of Aeronautics and Astronautics. Guide for the Verification and Validation of Computational Fluid Dynamics Simulations. AIAA G-077-1998, 1998.

Boemer, A., Qi, H. and Renz, U. Eulerian Simulation of Spontaneous Bubble Formation in a Fluidized Bed. Int. j. Multiphase Flow. vol. 23(5), page 927. 1998.

Boemer, A., Qi, H. and Renz, U. Verification of Eulerian Simulation of Bubble Formation at a Jet in a Two – Dimensional Fluidized Bed. Chemical Engineering Science, vol. 53, page 1835. 1998.

Demuren, A. O., Wilson, R. V. Estimating Uncertainty in Computations of Two-Dimensional Separated Flows, FED – Quantification of Uncertainty in Computational Fluid Dynamics, ASME, vol. 158, page 09. 1993.

Ergun, S. Fluid Flow through Packed Columns. Chemical Engineering Progress, vol.48(2), page 89, 1952.

Fluent inc., Fluent 6.2 User's Guide. Fluent 6.2 Documentation. 2005

Ferziger, J. H., Peric, M. Computational Methods for Fluid Dynamics, 2ª ed., Springer-Verlag, Berlin. 1999.

Gidaspow, D. Bezburuah, R., Ding J. Hydrodynamics of Circulating Fluidized Beds, Kinetic Theory Approach. 7th Engineering Foundation Conference on Fluidization - Proceeds, page 75, 1992.

Maliska, C., R. Transferência de Calor e Mecânica dos Fluidos, LTC, RJ, Brasil. 1995.

Marchi, C. H., Hobmeir, M. A.. Numerical Solution of Staggered Circular Tubes in Two-dimensional Laminar Forced Convection. J. of Braz. Soc. Of Mech. Sci. & Eng., Vol.29. 2007

Patil, D.J., van Sint Annaland, M. and Kuipers, J.A.M. Critical comparison of hydrodynamic models for gas–solid fluidized beds—Part I: bubbling gas–solid fluidized beds operated with a jet. Chemical Engineering Science, vol. 60. 2005.

Patil, D.J., van Sint Annaland, M. and Kuipers, J.A.M. Critical comparison of hydrodynamic models for gas–solid fluidized beds—Part II: freely bubbling gas–solid fluidized beds. Chemical Engineering Science, Vol. 60. 2005.

Roache, P. J. A Method for Uniform Reporting of Grid Refinement Studies. Quantification of Uncertainty in Computational Fluid Dynamics, vol. 158. ASME. 1993.

Roache, P. J. Verification and Validation in Computational Science and Engineering, Hermosa Publishers, New Mexico, USA. 1998.

Rosseto, M. Dispense A - Richiami e Integrazioni di Statistica. Corso di Sperimentazione e Affidabilità delle Costruzioni meccaniche, Politécnico di Torino, Itália. 2006.

Sinclar, J. L., Jackson, R. Gas-particle Flow in a Vertical Pipe with Particle-particle interactions. A.I.Ch,E. Journal 35, page 1473. 1989.

Sjögreen, B., Yee, H.C. Grid convergence of high order methods for multiscale complex unsteady viscous compressible flows. Journal of Computational Physics vol. 185, page1. 2003

Wen, C. Y., Yu, Y., H. Mechanics of Fluidization. Chemical Engineering Progress. Symp. Series, vol.62, page 100. 1966.

5. RESPONSIBILITY NOTICE

The authors are the only responsible for the printed material included in this paper.